The General Theory of the Quasi-Reproducible Experiments: How to Describe the Measured Data of Complex Systems?

The General Theory of the Quasi-Reproducible Experiments:

How to Describe the Measured Data of Complex Systems?

Raoul R. Nigmatullin[1,4],

[1)]Radio-electronics and Informative Measurements Technics Department,

Kazan National Research Technical University (KNRTU-KAI),

K. Marx str.10, Kazan 420011. Tatarstan, Russian Federation

Guido Maione, **Paolo Lino**, **Fabrizio Saponaro**[2)]

[2)]Department of Electrical and Information Engineering (DEI),

Politecnico di Bari, Via E. Orabona, 4, Bari, Italy

Wei Zhang[3,4)]

[3)]JiNan University(JNU),

College of Information Science and Technology,

Department of Electronic Engineering,

Guangzhou 510632, Guangdong, China

[4)]JNU-KNRTU(KAI) Joint Lab. of FracDynamics and Signal Processing,

JNU, Guangzhou, China

Abstract. In this paper, we suggest a general theory that enables to describe experiments associated with reproducible or quasi-reproducible data reflecting the dynamical and self-similar properties of a wide class of complex systems. Under complex system we understand a system when the model based on microscopic principles and suppositions about the nature of the matter is *absent*. This microscopic model is usually determined as "the best fit" model. The behavior of the complex system relatively to a control variable (time, frequency, wavelength, etc.) can be described in terms of the so-called *intermediate model* (IM). One can prove that the fitting parameters of the IM are associated with the amplitude-frequency response of the segment of the Prony series. The segment of the Prony series including the set of the decomposition coefficients and the set of the exponential functions (with $k = 1,2,\ldots,K$) is limited by the final mode K. The exponential functions of this decomposition depend on time and are found by the original algorithm described in the paper. This approach serves as a logical continuation of the results obtained earlier in paper [1] for *reproducible* experiments and includes the previous results as a partial case. In this paper, we consider a more complex case when the available data can create short samplings or exhibit some instability during the process of measurements. We give some justified evidences and conditions proving the validity of this theory for the description of a wide class of complex systems in terms of the reduced set of the fitting parameters belonging to the segment of the Prony series. The elimination of uncontrollable factors expressed in the form of the apparatus function is discussed.

To illustrate how to apply the theory and take advantage of its benefits, we consider the experimental data associated with typical working conditions of the injection system in a common rail diesel engine. In particular, the flow rate of the injected fuel is considered at different reference rail pressures. The measured data are treated by the proposed algorithm to verify the adherence to the proposed general theory. The obtained results demonstrate the undoubted effectiveness of the proposed theory.

List of acronyms:
IM – Intermediate Model
QR – Quasi-Reproducible
QP – Quasi-Periodical
CRIS – Common Rail Injection System
ECU – Electronic Control Unit
ET – Energizing Time
GPS – Generalized Prony Spectrum
LLSM – Linear Least Square Method
FLSM – Functional Least Square Method
PID – Proportional-Integral-Derivative

1. Introduction and formulation of the problem

The subject associated with treatment of data of different nature and from different fields or applications is today considered as well developed. It includes many books [2-10], a massive amount of papers (that cannot be enumerated here) and numerous conferences; they create a clearly expressed trend that is supported by many researches working in this field. The directed trend can be simply formulated: if an experimentalist has a set of accurately measured data obtained from a reliable equipment, then the problem of a theoretician is to find the microscopic/empirical model and to describe these data (after elimination of the influence of the apparatus function and random fluctuations) in terms of the fitting parameters that follow from the "best-fit" (microscopic) model. This is the basic tendency that forms a specific interaction between any theory and experiment and many researches follow and support this paradigm. In particular, non-trivial fractal model for description of the averaged motions in mesoscale was found [11]. It enables to describe a wide set of blow-like signals that can arise in many complex systems. Here we should mark the recent review paper [12] totally dedicated to consideration of different methods used in analysis of complex systems. The active interest in investigation of properties of many complex systems where the microscopic model cannot be created allows us to put forward the following problem: *is it possible to formulate a general theory based on an intermediate model (IM) for description of the*

properties of a wide class of complex systems in one unified scheme? This intermediate model should present a "universal" platform containing the reduced set of the fitting parameters which can describe the measured data of the considered complex system with high accuracy in order to compare different responses (measured data) in one unified scheme. If this platform can be created, then it will present an interest for the theoreticians as well. Namely, any theory (or suggested microscopic model) expressed in the parameters of the IM will be compared with experimental data that are expressed also in the *same* set of the fitting parameters. This unified scheme detects possible errors that are admitted by both sides to achieve the true coincidence between the competitive theory and data cleaned from the influence of the apparatus and other distortions.

We want to prove that an "ideal" IM can be presented by the segment of the Fourier series, F-series for short, in the case of the "ideal" experiment [1], or by the segment of the generalized Prony series. Below, it will be proved that the IM can be presented by a function of the type

$$F(t) = \left[\kappa_1(t)\right]^{t/T} \mathrm{Pr}_1(t) + \left[\kappa_2(t)\right]^{t/T} \mathrm{Pr}_2(t), \tag{1}$$

where T is a mean period of time between two successive measurements, $\mathrm{Pr}_{1,2}(t)$ and $\kappa_{1,2}(t)$ are periodic functions with respect to the value of T. These functions can be presented by the segments of the F-series

$$\begin{aligned} &\mathrm{Pr}_{1,2}(t \pm T) = \mathrm{Pr}_{1,2}(t),\ \kappa_{1,2}(t \pm T) = \kappa_{1,2}(t), \\ &\Phi(t) = A_0 + \sum_{k=1}^{K} \left(Ac_k \cos\left(2\pi k \frac{t}{T}\right) + As_k \sin\left(2\pi k \frac{t}{T}\right) \right). \end{aligned} \tag{2}$$

The function $\Phi(t)$ is associated with any periodic function figuring in expression (1). The coefficients of this F-series (including the coefficient A_0, the mean value of T and the value of the final mode K) form the set of the desired fitting parameters (Ac_k, As_k, k = 1,2,…,K) that can describe the response of the analyzed complex system. The periodic functions $\kappa_{1,2}(t)$, under reasonable suppositions described below, express the influence of the apparatus function and the procedure of its elimination reduces the IM to the segment of F-series

$$F(t) = \mathrm{Pr}_1(t) + \mathrm{Pr}_2(t),\ F\left(t \pm T\right) = F(t), \tag{3}$$

that corresponds to an "ideal" experiment, when all measurements are becoming *identical* to each other. This problem is a logic continuation of the previous investigation that produced the results shown in paper [1], where the approximate expression (1) for the case $\kappa_1(t) = \lambda_1, \kappa_2(t) = \lambda_2, \lambda_{1,2} = const$ was obtained. In comparison with equation (12) considered in [1] (see also equation (4) below), we put the constant b = 0 and consider the simple case L = 2, when the memory between measurements is short. The equation (1) describes also a more complex case, when the measured data are *quasi-reproducible* (i.e. they can be varied during the measuring

process). Earlier, it was supposed that these measurements are relatively stable (reproducible). The applicability of this general theory and its possible limitations will be discussed in the last section.
The structure of this paper is organized as follows. In the second section, we give the basics of the new theory, the third section is related to the description of important details associated with experimental measurements that are used for confirmation of this theory. The fourth section contains the algorithm and describes the basic treatment stages that can be also applied to data obtained from other complex systems. The fifth section is related to discussion of the obtained results and to further steps that will be useful and constructive for further research.

2. The basics of the general theory related to the treatment of reproducible data

In paper [1] the general theory of experiments containing reproducible data was considered. The basic equation that was confirmed earlier on available data [12-14]

$$F(x+LT_x)=\sum_{l=0}^{L-1}a_l F\left(x+lT_x\right), \tag{4}$$

reflects the existence of the strong correlations (memory) between successive measurements. Here x is the input ("control") variable, which can coincide with time, frequency, wavelength or another external factor. T_x as before is identified with the mean period of this variable between successive measurements. Mathematically, this memory between measurements is expressed by a set of constants a_l (l = 0,1,…,L-1) which, in turn, are found easily from (4) by the linear least square method (LLSM). This supposition is verified as correct when we have relatively large sampling (number of measurements M > 100) and stable measurements that are statistically close to each other. In case of strong influence by uncontrollable factors, this approximate supposition is *not* valid and we should consider a more complex case when the set of the parameters $a_l(x)$ are the functions of the input variable x. We define this case (when the measured data can be significantly varied) as quasi-reproducible (QR). So, we should consider the functional equation

$$F(x+LT_x)=\sum_{l=0}^{L-1}a_l(x)F\left(x+lT_x\right), \tag{5}$$

which includes the previous functional equation as a partial case. We omit here the additive constant b figuring earlier in equation (4) (see [1]). In order to find the solution of the functional equation (5) in analytical form, we *suppose* that the set of the functions $a_l(x)$ are periodical with respect to T_x i.e. $a_l(x \pm T_x) = a_l(x)$. Another obstacle is related to the fact that these functions are *not* known and can be derived only from the set of quasi-periodic (QP) measurements. We show how to find them for the simple case in which the memory is limited to the previous two (L=2) experiments:

$$F_{m+2}(x) = \langle a_1(x) \rangle F_{m+1}(x) + \langle a_0(x) \rangle F_m(x),$$
$$F_m(x) \equiv F\left(x + mT_x\right),\ m = 1,...,M \tag{6}$$

Here the index m determines the set of the successive measurements, while the unknown functions $<a_1(x)>$ and $<a_0(x)>$ can be obtained from the averaging procedure (described below) based on available data and they are supposed *not* having dependence on m. To find them, we multiply (6) by the functions $F_{m+1}(x)$, $F_m(x)$, correspondingly, and then take the average value over all the admissible measurements. We introduce the pair correlation function of the type

$$K_{sq}(x) = \frac{1}{M-s}\sum_{m=1}^{M-s} F_{m+s}(x) F_{m+q}(x),$$
$$q = 0,1,\ s = 2. \tag{7}$$

After realization of this procedure with the functions $F_{m+1}(x)$ and $F_m(x)$ in equation (6) we obtain

$$K_{21}(x) = \langle a_1(x) \rangle K_{11}(x) + \langle a_0(x) \rangle K_{10}(x)$$
$$K_{20}(x) = \langle a_1(x) \rangle K_{10}(x) + \langle a_0(x) \rangle K_{00}(x)$$
$$K_{2,q} = \frac{1}{M-2}\sum_{m=1}^{M-2} F_{m+2}F_{m+q},\ K_{q,q} = \frac{1}{M-2}\sum_{m=1}^{M-2} F_{m+q}F_{m+q} \tag{8}$$
$$q = 0,1.$$

From this system of linear equations one can easily find the desired unknown functions $<a_1(x)>$ and $<a_0(x)>$. General approach and justification of this procedure (expressed by relationships (8)) are considered in Appendix 1.

Coming back to (6), we are looking for the solution of this equation in the form

$$F_m(x) = \left[\kappa(x)\right]^{x/T_x} \Pr(x),$$
$$\kappa\left(x \pm T_x\right) = \kappa(x), \Pr(x \pm T_x) = \Pr(x). \tag{9}$$

Substitution of expression (9) into equation (6) leads to the following quadratic equation

$$\kappa^2(x) - \langle a_1(x) \rangle \kappa(x) - \langle a_0(x) \rangle = 0$$
$$\kappa_{1,2}(x) = \frac{\langle a_1(x) \rangle}{2} \pm \sqrt{\left(\frac{\langle a_1(x) \rangle}{2}\right)^2 + \langle a_0(x) \rangle} \tag{10}$$

So, the solution of equation (6) is written in the form (1), where the function $F(x)$ (at m = 0) coincides with an "initial" measurement $F_0(x)$ and the unknown periodic functions $Pr_{1,2}(x)$ should be presented in the sense of the segments of the F-series (2). In practice, it is preferable to operate with small samplings when M >3. How to apply equation (6) in this case? For M > 3, we use an idea that has been applied in the previous papers [1, 12-14]. In brief, this idea helps to divide all measurements on three groups relatively to the slopes Sl_m belonging to each measurement (m)

which are calculated, in turn, with respect to the mean measurement. Really, let us define these slopes as

$$Sl_m = slope(\langle y\rangle, y_m) = \frac{\left(y_m \cdot \langle y\rangle\right)}{\left(\langle y\rangle \cdot \langle y\rangle\right)}, \qquad \langle y\rangle = \left(\frac{1}{M}\right)\sum_{m=1}^{M} y_m,\ (A\cdot B) = \sum_{j=1}^{N} A_j B_j \tag{11}$$

Here we give the conventional definition of the slope between the current measurement y_m and the mean measurement <y>. The parenthesis determines the scalar product between two functions having j=1,2,…,N measured data points. Here we *suppose* that the initial measurements $y_m(x)$, for m = 1,…, M, coincide approximately with functions $F_m(x)$ ($y_m(x) \cong F_m(x)$) figuring in the functional equation (6). If we construct the plot Sl_m as a function of the successive measurement (m) and rearrange all measurements in the descending order $SL_1 > SL_2 > \ldots > SL_M$, then all measurements can be divided in three groups. The "up" group has the slopes located in the interval (1+Δ, SL_1), the mean group (denoted by "mn") with the slopes in (1-Δ, 1+Δ), and the down group (denoted by "dn") with the slopes in (1-Δ, SL_M). The value Δ is chosen for each QP experiment separately. This curve has a great importance and reflects the quality of the realized successive measurements and the used equipment. Preliminary analysis realized on many available data allows to select three different cases. They are shown in Figs. 1(a,b,c). The bell-like curve (that can be fitted with the help of four fitting parameters α, β, A, B) is described by the beta-function

$$Bd(m;\alpha,\beta,A,B) = A\left(m\right)^{\alpha}\left(M-m\right)^{\beta} + B\,, \tag{12}$$

and reflects the quality of the realized measurements. The straight line (it can have a slope) divides all measurements in three groups: (a) the beginning point of a bell-like curve up to the first intersection point determines the number *Nup* of measurements in the “up” group and is characterized by the *Yup*(x) curve; (b) the region between the two intersection points determines the number *Nmn* of measurements in the “mn” group with slope close to one and characterized by the set of measurements forming the curve *Ymn*(x) and, finally, (c) the rest of the measurements *Ndn* in the “dn” group is covered by the curve *Ydn*(x). If the number of measurements *Nmn* > *Nup*+*Ndn* then these measurements are characterized as "good", in the case when *Nmn* ≈ *Ndn* ≈ *Nup* the measurements (and the corresponding equipment) are characterized as "acceptable", and the case when *Nmn* < *Nup* + *Ndn* is characterized as "bad". Quantitatively, all three cases can be characterized by the ratio

$$Rt = \left(\frac{Nmn}{Nup + Ndn + Nmn}\right)\cdot 100\% = \left(\frac{Nmn}{M}\right)\cdot 100\% \tag{13}$$

In the expression (13), *M* determines the total number of measurements. Based on this ratio one can determine easily three classes of measurements: "good" when 60% < *Rt* < 100%, "acceptable" when 30% < *Rt* < 60%, and "bad" when 0 < *Rt* < 30%. This preliminary analysis is supported by Figs.1(a, b, c).

Coming back to expression (10), we make the following remark. If the function $\kappa_1(x)$ is always positive ($\kappa_1(x) > 0$) and, correspondingly, the function $\kappa_2(x)$ is negative ($\kappa_2(x) < 0$) for all values of the *input* variable *x* then the solution is rewritten in the form

$$
\begin{aligned}
&F_0(x) = \left[\kappa_1(x)\right]^{x/T_x}\,\mathrm{Pr}_1(x) + \left[\left|\kappa_2(x)\right|\right]^{x/T_x}\,\mathrm{APr}_2(x),\\
&\mathrm{Pr}_1(x \pm T_x) = \mathrm{Pr}_1(x),\ \mathrm{APr}_2(x \pm T_x) = -\mathrm{APr}_2(x).\\
&\mathrm{Pr}_1(x) = \sum_{k=1}^{K}\left(Ac_k^{(1)}\cos\left[\left(2k\right)\pi\frac{x}{T_x}\right] + As_k^{(1)}\sin\left[\left(2k\right)\pi\frac{x}{T_x}\right]\right)\\
&\mathrm{APr}_2(x) = \sum_{k=1}^{K}\left(Ac_k^{(2)}\cos\left[\left(2k-1\right)\pi\frac{x}{T_x}\right] + As_k^{(2)}\sin\left[\left(2k-1\right)\pi\frac{x}{T_x}\right]\right)
\end{aligned}
\qquad (14)
$$

Expressions (14) demonstrate the final result that can be tested on real data. In comparison with the previous case [1], all quasi-reproducible (QR) data depend only on two initial measurements $F_0(x)$ and $F_1(x)$ that can be corrected by the functions (10) and the recurrence relationship (6) for other measurements. We do not give the corresponding formulae that can be associated with an "ideal" experiment [1]. In this complex case, the pure periodic function cannot be extracted easily. It can be a linear combination of periodic, anti-periodic or other more complex combinations. In the case of strong data variability, the elimination of the "apparatus" function, i.e. the influence of the experimental equipment, needs a special consideration in each partial case. If we reduce the *M* measurements to three averaged measurements $F_2(x) = Yup(x)$, $F_1(x) = Ydn(x)$, $F_0 = Ymn(x)$ then we have the relationship

$$
\begin{aligned}
&F_2(x) = \left\langle a_1(x)\right\rangle F_1(x) + \left\langle a_0(x)\right\rangle F_0(x),\\
&F_2(x) \equiv Yup(x) = \frac{1}{Nup}\sum_{m=0}^{Nup-1} y_m(x),\\
&F_1(x) \equiv Ydn(x) = \frac{1}{Ndn}\sum_{m=0}^{Ndn-1} y_m(x),\\
&F_0 \equiv Ymn(x) = \frac{1}{Nmn}\sum_{m=0}^{Nmn-1} y_m(x).
\end{aligned}
\qquad (15)
$$

In expression (15) each summation includes the *different* measurements $y_m(x)$ that enter in three independent groups "up", "mn" and "dn" in accordance with the "slopes" criterion defined by expressions (11)-(13). These three artificially created measurements added to the initial set of measurements do not change essentially the values of the mean functions $<a_1(x)>$, $<a_0(x)>$.

3. The experimental set-up

In this section, we illustrate the real system considered to produce data from experimental measurements. The system is a Common Rail Injection System (CRIS), which is currently the main fuel delivery system that is used in automotive industry for light/heavy-duty Diesel engines (see Figure 2). The aim of CRIS is to meter the injected fuel amount and to optimize the fuel/air ratio into the cylinders for an optimal combustion process. The CRIS can be divided into three basic circuits and related components: the low-pressure supply circuit (fuel tank, low-pressure pump), the high-pressure delivery circuit (high-pressure pump, common rail, injectors), and a backflow circuit in which the excess fluid returns to the tank.

The injection process is managed by a control module within an Electronic Control Unit (ECU) that ensures, in the entire operating range, a stable high pressure level in the common rail and a proper amount of fuel to be injected according to the engine demand.

In the load mode, when the vehicle accelerator pedal is pressed down and a specific engine torque is requested, the ECU calculates the required fuel injection quantity and the rail pressure set-point to reach from a combination of pre-established basic maps. The low-pressure pump sends the fuel coming from the tank to the pump chamber of the high-pressure pump. Thanks to the radial pistons driven by the camshaft, the high-pressure pump allows to increase the pressure and feeds the common rail through a delivery valve. The rail pressure raises to reach the reference set-point and to hydraulically feed the injectors. During the injection phase, a reference voltage of a given duration indicated by ET (Energizing Time) is applied to the solenoid valve of the electro-injector, which indirectly determines the lift of a plunger-needle mechanical coupling inside the injector, then the injection of fuel into the cylinder through the nozzles. An open-loop pre-control (for the steady-state response) and a closed-loop PID (Proportional-Integral-Derivative) control (for the transient response) are implemented in the ECU to ensure pressure regulation and a fast response with limited overshoots and undershoots with respect to the set-point. According to the actual rail pressure, which is acquired by a dedicated sensor, the leakage flow and the injection quantity, the ECU controls the lamination of the excess flow towards the backflow circuit in three ways depending on the operating conditions: a) by the metering control valve within the high-pressure pump; b) by the pressure control valve in the rail; c) and by a combination of both.

To reduce energy consumption, noise, and pollutant emissions, while ensuring high-level performance indexes, an engine test bench with a proper measurement instrumentation is required to calibrate the controller parameters and to evaluate the response of the main variables. In particular, the injected flow rate is one of the most important quantities to acquire with high accuracy.

Namely, properly shaping the flow rate strongly affects the combustion process and therefore the overall performance.

The electro-injector is analyzed and characterized on the test bench at several operating conditions: the set-point values of the rail pressure can be 300, 800, 1200, 1600 [bar]; ET can be 300, 700, 1300 [μs]. The injected flow rate Q_{inj} is measured by the Bosch Rate of Injection Meter [13-16] by means of the pressure wave that is produced by the injection into a length of compressible fluid. The meter (Figure 3) consists of an injector housing, a measuring tube, an orifice, and a check valve. The injector housing allows to force the injector tip at the beginning of the measuring tube and to acquire the pressure waves by the strain gages. A variable orifice plate is positioned in the middle of the measuring tube to determine the reflected pressure waves and the transmitted pressure waves to the second part of tube. The inside diameter and the length of the measuring tube determines the magnitude of the pressure waves and the attenuation efficiency of the meter respectively. The check valve located at the end of the tube adjusts the back pressure to the reference.

The injected flow rate is obtained from the pressure-velocity equation in a non-stationary flow condition:

$$P = c\,\rho\,u, \tag{16}$$

where P is the pressure, c is the speed of sound in the fluid, ρ is the density of the fluid and u is the flow velocity. Combined with the continuity equation, the injected flow rate is derived as:

$$Q_{inj} = \frac{dV}{dt} = \frac{A}{c\,\rho}P, \tag{17}$$

where V is the volume of fuel and $\frac{dV}{dt}$ is the volumetric flow rate.

The time resolution is related to the data acquisition system (< 1μs) and to the pressure transducer, while the sensitivity is about 0.1 mg/stroke.

4. The processing of the measured data in the frame of the unified scheme

The basic aim of this paper is to show the application of the general approach to the treatment of real data related to the complex system illustrated in the previous section. We consider the injection flow rate data taken at the fixed reference rail pressure of 800 bar and for the three fixed values of the energizing time (ET): 300μs, 700μs, 1300μs. For each value of ET, M = 100 experimental flow rates are measured: y_1 [mm^3/ms] , ... , y_{100} [mm^3/ms], each occupying a time length (injection duration) of 8.3 ms and with sample time of 5μs. In order to understand clearly the general approach, we divide the whole treatment procedure in some stages that play an important role in the possible application to other kinds of data.

Stage 1. *The separation of all measurements in three mean curves*

We illustrate this stage by the Fig. 4. Here we show some randomly taken measurements representing all the set (M=100) as the function of time in the interval [0, 8.3 10^{-3}] s and with respect to their mean function $<y>$. The plot shown above in Fig. 4 demonstrates strong correlations between measurements. The distribution of the slopes (see equation (11)) for all measurements m (m = 1,2,…,M) is shown on Fig. 5(a). We select approximately the value of Δ=1/3 and divide the span between the ordered measurements (the curve SL) in three parts: "up" with ($1+\Delta_{up}$, max(SL)), "mn" with ($1-\Delta_{dn}$, $1+\Delta_{up}$), "dn" with (min(SL), $1-\Delta_{dn}$,), where Δ_{up} = [max(SL)-1]/3 and Δ_{dn} = [1-min(SL)]/3. The numbers of measurements that are located in each selected interval are Nup = 11, Nmn = 65, Ndn = 24. This procedure is shown also on Fig.5(a). After subtraction of the unit value and the subsequent integration, we obtain the bell-like curve shown on Fig.5(b). The quality of measurements calculated in accordance with expression (13) is equal to Rt = 65%. Clusterization realized with the help of expression (15) helps to receive only three mean curves *Yup*, *Ydn*, *Ymn* shown on Fig.6. These averaged curves can be added to the previous set of measurements. The realization of the procedure described by expressions (7) and (8) shows that the values of the averaged constants $<a_{0,1}(x)>$ are practically unchanged.

Stage 2. *Reduction to three incident points*

If one looks at these three mean curves *Yup*, *Ydn*, *Ymn*, they still contain high-frequency (HF) fluctuations. To decrease their influence, we apply the procedure defined as the reduction to three incident points. This procedure was successfully applied to many random functions [17-21] proving their self-similar (fractal) properties. We choose s = 1,2,…,b=16 points (Y_1,Y_2,…,Y_b) and reduce them to three incident points (max(Y), mean(Y), min(Y)) by keeping them invariant relatively to the permutations inside the chosen b points. Having in mind the total number of data points L=1660 and the length of a small "cloud" of points b = 16, we obtain the reduced number R of data points as the integer part of [L/b] (R=100), by keeping the form of the initial curve almost unchanged relatively to this transformation. The result of the reduction procedure is shown on Fig.7. If one compares the curves depicted on Fig.6 and *Ymn* depicted on the upper plot of Fig.7, then they are similar to each other. The calculations of the functions $\kappa_{1,2}(t)$ by the formulae (7)-(10) are shown on Fig.8. Direct application of the reduction procedure to these functions is *impossible* because the HF fluctuations destroy completely the self-similar property [18,20]. In order to restore this property and then apply the reduction procedure, we should smooth preliminary the functions $\kappa_{1,2}(t)$. They are shown on Fig. 8 by bold lines. These smoothed functions can be reduced again and after reduction we obtain the reduced functions $r_{1,2}(x)$ from the smoothed roots. These functions are shown on Fig.8 above.

Stage 3. *The fitting of the mean reduced function*.

The previous stages have a preparatory character. The basic result will be obtained when we fit the reduced function $Y(x)$ ($Y = Mn$, $x = tmn$) to the function (14). For convenience we rewrite this function in the form

$$Y(x) \cong F(x;K,T_x) = A_0 E_0^{(1)}(x) + \sum_{k=1}^{K}\left(Ac_k^{(1)}Ec_k^{(1)}(x) + As_k^{(1)}Es_k^{(1)}\right) + \sum_{k=1}^{K}\left(Ac_k^{(2)}Ec_k^{(2)}(x) + As_k^{(2)}Es_k^{(2)}\right),$$

$$E_0^{(1)}(x) = \left[r_1(x)\right]^{x/T_x},\ Ec_k^{(1)} = \left[r_1(x)\right]^{x/T_x}\cos\left(2\pi k\frac{x}{T_x}\right), Es_k^{(1)} = \left[r_1(x)\right]^{x/T_x}\sin\left(2\pi k\frac{x}{T_x}\right), \quad (18)$$

$$Ec_k^{(2)} = \left[\left|r_2(x)\right|\right]^{x/T_x}\cos\left(\pi(2k-1)\frac{x}{T_x}\right), Es_k^{(2)} = \left[\left|r_2(x)\right|\right]^{x/T_x}\sin\left(\pi(2k-1)\frac{x}{T_x}\right).$$

Here the known functions $r_{1,2}(x)$ should be associated with the reduced values of the smoothed roots $\kappa_{1,2}(t)$, The functions $Ec_k^{(2)}(x), Es_k^{(2)}(x)$ take into account the fact that the root $r_2(x)$ is *negative*. The function $F(x;\ K,\ T_x)$ contains only two nonlinear fitting parameters that can be found from the minimization of the relative error surface

$$\min\left[RelError\left(\frac{stdev\left(Y(x)-F(x;K,T_x)\right)}{mean\left(\left|Y(x)\right|\right)}\right)\cdot 100\%\right], \quad (19)$$

that are given by (K, T_x). Usually, T_x is not known and lies in the interval ($0.5T_{in} < T < 2T_{in}$), $T_{in} = (x_1 - x_0)\cdot\text{length}(x)$. The minimal value of the final mode K is found from the condition that the level of the relative error should be located in the interval (1% – 10%). After minimization of the value (19), the amplitudes $A_0, Ac_k^{(1,2)}(x), As_k^{(1,2)}(x)$ are found by the LLSM.

The result of application of this procedure is shown on Fig. 9. The quality of the fitting curve (18) is very high because the number of the amplitudes $4K$=104 is comparable with number of the reduced points R=100. The total distribution of amplitudes is shown by the figure 10(a). Actually, this distribution together with other fitting parameters (shown in the Table 1) represents itself the desired IM. We should stress also the importance of the bell-like curve (Fig. 10(b)) that serves as a useful tool for analysis of spectrograms containing large number of the discrete amplitudes (>100). The separated distributions of the amplitudes $Ac_k^{(1,2)}(x), As_k^{(1,2)}(x)$ are shown on Figs. 10(c).

In the same manner, we can treat other files corresponding to P = 800 bar but with other values of the energizing time (ET) that are equal to 700 μs and 1300 μs. In order not to overload the context by a large number of figures, we give only the important ones: (a) the distribution of the slopes (expressed in the form of bell-like curves) that demonstrate the quality and stability of the measurements performed for each value of ET (see Fig. 11); (b) the fit of the reduced curves for the values of ET equal to 700 μs and 1300 μs. The fitting curve for 300 μs cannot be placed together with these two ones because it has a small scale (see Fig.12); (c) the total distribution of all amplitudes expressed in the form of bell-like curves for 3 values of ETs for their comparison (see

Fig.13(a)). The separate distributions of the amplitudes $Ac_k^{(1,2)}(x), As_k^{(1,2)}(x)$ for 700 μs and 1300 μs are presented by Figs. 13(b, c). Additional values of the fitting parameters for all ETs are collected in the Table.

5. Results and discussion

In this paper, we suggest the general theory for description of the QR-data and the finding of the fitting function that is defined as the IM. This IM is expressed in the form of the finite segment of the generalized Prony spectrum (GPS). All quantitative parameters characterizing the given random function $Y(x)$ can be expressed in the form of the GPS. Schematically, it can be written as

$$Y(x) \to \left\{ \kappa(t),\, T_x, A_0, K, Ac_k^{(1,2)}, As_k^{(1,2)} \right\} \tag{20}$$

The functions characterizing the roots $\kappa(t)$ can be also presented by the segment of the F-series, because of their periodicity. Other parameters of the IM for the specific experimental situation considered in paper are determined by expression (18). If necessary, one can add also 4 fitting parameters characterizing the behavior of the bell-like curve (12) that describes the quality of the realized measurements. All these fitting parameters describe quantitatively the suggested IM.

Actually, this IM can be used as the general platform were the properties of different complex systems can be analyzed and compared with each other in the frame of the unified scheme. All theoretical functions that follow from the microscopic/empirical theory (defined in this paper as the "best-fit" theory) can be presented also as a segment of the generalized Prony decomposition and compared with experimental measurements on the basic of this general platform. In comparison with the previous version [1], the more general variant presented in this paper takes into account the temporal dependence of the exponential functions $\exp\left(\left(t/T\right)\cdot\ln\left(\kappa_{1,2}(t)\right)\right)$ that increases essentially the region of its applicability and allows to consider the so-called "quasi-reproducible" experiments, where the influence of uncontrollable external factors during the process of measurements are essential (chemical experiments, biological measurements, etc.).

Attentive researchers may pose the following question: if the authors pretend on some generalization of the conventional theory of measurement, then is it possible to consider a more general relationship in comparison with supposition (6) and realize the forecasting procedure, if the IM is supposed to be found? In other words, is it possible to extend the observations out of the admissible interval if the fitting function in the given interval is known? The answers on these posed questions are considered in Appendices 1 and 2. Another important question is related to application of this general theory for the short samplings. We deliberately considered the case when the number of measurements is relatively high (M=100) but for some unreproducible data the

number of measurements can be small. The approach suggested in this paper allows to consider the case when we have a minimal number of measurements. Imagine that we do not have sufficient number of measurements and the allowed number of measurements M=3. What we should do in this "unpleasant" case? Coming back to (6) we have

$$\begin{aligned} &F_3(x) = \langle a_1(x) \rangle F_2(x) + \langle a_0(x) \rangle F_1(x), \\ &F_m(x) \equiv F\left(x + mT_x\right),\ m = 1,2,3 \end{aligned} \tag{21}$$

The expression (8) remains valid but for M=3 we obtain

$$\begin{aligned} &K_{32}(x) = \langle a_1(x) \rangle K_{22}(x) + \langle a_0(x) \rangle K_{21}(x) \\ &K_{31}(x) = \langle a_1(x) \rangle K_{21}(x) + \langle a_0(x) \rangle K_{11}(x) \\ &K_{32} = F_3F_2,\ K_{31} = F_3F_1,\ K_{22} = \left(F_2\right)^2, \\ &K_{21} = F_2F_1,\ K_{11} = \left(F_1\right)^2. \end{aligned} \tag{22}$$

One can show that the functions $\langle a_{1,0}(x) \rangle$ are reduced to the constants $A_{1,0}$ that can be calculated with the help of the LLSM. The justification of expressions (8) and (21) associated with coupling of the measured functions is proved in Appendix 1. So, this observation allows to correct the definition of the term quasi-reproducible data. Under the QR-data one can understand the data when the influence of the uncontrollable factors are essential and should be taken into account (in the form of the temporal dependence of the roots $\kappa_{1,2}(t)$) and the number of measurements $M \geq 3$. But what about the rare and unique events when M=1? This question remains still open and is needed in the further research.

The nontrivial example of the chosen complex system associated with consideration of the CRIS functioning shows that all peculiarities (including the desired fit of the basic characteristics (see Figs. 9,12) can be expressed in terms of the common fitting parameters that follow from the proposed approach. Similarly, one can consider another system. We omit the consideration of the system studied for other values of the input parameters P = 800, 1200, 1600 [bar]; ET = 300, 700, 1300 [μs] in order not to overload the essence of this theory by large numbers of figures and similar details. Probably, all specific details associated presumably with the CRIS functioning will be a subject of the further research.

The proposed general theory can receive a wide propagation in various practical applications. In the end of this section, from our point of view, we want to remind at least a couple important problems that can be solved with the help of this approach.

1. Creation of a fully computerized laboratory. Really many routine experiments can be completely computerized and finally present all measured random functions in terms of the fitting parameters belonging to the IM. Any "best-fit" theory pretending for explanation of these phenomena should be expressed in terms of the fitting parameters belonging to the IM, also. The proper comparison of the

IM with the specific model can give a significant impact for more deeper understanding of the studied phenomenon.

2. Creation of a unified metrological standard. Any attentive reader had a chance to notice that any measured "quality" can be expressed quantitatively in terms of the fitting parameters belonging to the GPS. It signifies that any precise measurements characterizing the pattern equipment can serve as the unified metrological standard for comparison of the same type of product (unifying different equipments/instruments) with the product that was chosen as the pattern one. The GPS facilities also the complete product acceptance when any tested product is compared with the pattern product. If the unified standard determines the acceptable range of parameters received from the pattern product for the party of the tested product, then all process can be organized automatically in accordance with the "traffic light" principle. All acceptable products will pass on the "green" light, while the abandoned product marked by "red light" can be a subject of analysis of the qualified personnel.

Appendix 1.

The functional least square method (FLSM) and the general solution for the functions <$a_l(x)$>

In this section, we consider the more complex case when the memory between successive measurements is relatively long and occupies L independent measurements. For this case we have

$$F_{L+m}(x) = \sum_{l=0}^{L-1} \langle a_l(x) \rangle F_{m+l}(x) \qquad \text{(A1-1)}$$

As before, the functions $\langle a_l(x \pm T) \rangle = \langle a_l(x) \rangle$ are supposed to be periodic with mean period T. How to find the unknown functions $\langle a_l(x) \rangle$ in this general case for any L? We require that the quadratic dispersion between the left and the right sides of expression (A1-1) should be minimal

$$\sigma(x) = \left(F_{L+m}(x) - \sum_{l=0}^{L-1} \langle a_l(x) \rangle F_{m+l}(x) \right)^2 = \min \qquad \text{(A1-2)}$$

Taking the *functional* derivatives of the function σ(x) with respect to the functions $\langle a_l(x) \rangle$ and equating each partial derivative to zero we have

$$-\frac{\delta\sigma(x)}{\delta \langle a_s(x) \rangle} = \sum_{m=1}^{M-L} F_{s+m}(x) \cdot \left(F_{L+m} - \sum_{l=0}^{L-1} \langle a_l(x) \rangle F_{l+m}(x) \right) = 0 \qquad \text{(A1-3)}$$

In the last expression we added also the averaging procedure over all admissible measurements (m=1,2,…, M–L) because the unknown functions $\langle a_l(x) \rangle$ do not depend on index m. After introducing the notations

$$K_{L,s}=\frac{1}{M-L}\sum_{m=1}^{M-L}F_{L+m}(x)F_{s+m}(x),\ K_{l,s}=\frac{1}{M-L}\sum_{m=1}^{M-L}F_{l+m}(x)F_{s+m}(x),$$
$$l,s=0,1,...,L-1 \qquad \text{(A1-4)}$$

from (A1-3) we obtain the system of equations for the finding of unknown functions

$$\sum_{l=0}^{L-1}K_{l,s}(x)\langle a_l(x)\rangle=K_{L,s}(x),$$
$$s=0,1,...,L-1. \qquad \text{(A1-5)}$$

So, here we obtained the important result: the generalization of the LLSM for the finding of the unknown set of the functions $\langle a_l(x)\rangle$, which is natural to define as the *functional* least square method (FLSM). In the partial case for L=2 this general result is reduced to expression (8). It is instructive also to obtain the result for L=1. For this simple case we have

$$F_{m+1}(x)=\langle a_0(x)\rangle F_m(x)+b(x),$$
$$m=0,1,...,M. \qquad \text{(A1-6)}$$

Here we *suppose* that the function $b(x)$ is periodical (i.e. $\langle b(x\pm T)\rangle=\langle b(x)\rangle$. From the general expression we have

$$K_{10}(x)=\langle a_0(x)\rangle K_{00}(x)+b(x)\langle F_0(x)\rangle,$$
$$\langle F_1(x)\rangle=\langle a_0(x)\rangle F_0(x)+b(x).$$
$$K_{10}(x)=\frac{1}{M-1}\sum_{m=1}^{M-1}F_{1+m}(x)F_m(x),\ K_{00}(x)=\frac{1}{M-1}\sum_{m=1}^{M-1}F_m(x)F_m(x), \qquad \text{(A1-7)}$$
$$\langle F_1(x)\rangle=\frac{1}{M-1}\sum_{m=1}^{M-1}F_{1+m}(x),\ \langle F_0(x)\rangle=\frac{1}{M-1}\sum_{m=1}^{M-1}F_m(x),\ \langle F_1(x)\rangle\neq\langle F_0(x)\rangle.$$

From the system of linear equations (A1-7) one can find easily the unknown functions <$a_0(x)$> and $b(x)$. The solution of the functional equation (A1-6) for the conditions mentioned above is written in the form

$$F_0(x)=\left[\kappa(x)\right]^{x/T_x}\Pr(x)+C(x),$$
$$\kappa(x)=\langle a_0(x)\rangle,\ C(x)=\frac{b(x)}{1-\kappa(x)},\ \kappa(x)\neq 1, \qquad \text{(A1-8)}$$
$$F_0(x)=\Pr(x)+b(x)\frac{x}{T_x},\ \kappa(x)=1.$$

The function $F_0(x)$ can be associated with the initial measurement. Other functions $F_m(x)$ (m =1,2,…,M) can be restored from expression (A1-6). Finishing this section it is necessary to write the solution of the functional equation (A1-1) for the case when the functions are supposed to be periodical $\langle a_l(x\pm T)\rangle=\langle a_l(x)\rangle$. We are looking for the solution in the form

$$F_0(x)=\left[\kappa(x)\right]^{x/T_x}\Pr(x), \qquad \text{(A1-9)}$$

where, as before $\Pr(x \pm T_x) = \Pr(x)$. Inserting this trial solution in (A1-1) we obtain

$$\left[\kappa(x)\right]^L - \sum_{l=0}^{L-1} \langle a_l(x) \rangle \left[\kappa(x)\right]^l = 0, \tag{A1-10}$$

which is the equation for the finding of the desired functions $\kappa_q(x)$, $q = 1, 2, ..., L$. So, the general solution of the functional equation (A1-1) for the initial function $F_0(x)$ can be finally written in the form

$$F_0(x) = \sum_{q=1}^{L} \left[\kappa_q(x)\right]^{x/T_x} \Pr_q(x) \tag{A1-11}$$

Other solutions for m=1,2,…,M can be found easily from (A1-11)

$$F_s(x) \equiv F(x + sT_x) = \sum_{l=1}^{L} \left[\kappa_l(x)\right]^{s+\frac{x}{T_x}} \Pr_l(x). \tag{A1-12}$$

The last expressions (A1-11, 12) can be defined as the generalized Prony series (GPS) because the exponential factor figuring before the periodic function is the function of input variable x.

Appendix 2.

How to find the behavior of the fitting function out of the measurement interval [0, T_x]?

We want to show here that the general solution (A1-11) solves another important problem as *prediction* of behavior of the measured function $F(x)$ out of the interval of observation of the input/control variable x. Imagine that the measured data are fitted properly in the frame of the model (A1-11) and that the aim is to continue this fit out of the interval [0, x] adding some shift Δ to the admissible interval $0 \le x \le T_x + \Delta$. *Is it possible to solve this problem in the same frame of the introduced general concept or not?* From the mathematical point of view, it is necessary to express the function $F(x + \Delta)$ with the help of the function $F(x)$ by reducing the new interval of observation to the previous one. The solution expressed in the form of (A1-11) *admits* this separation:

$$\begin{aligned}
&F_0(x) = \sum_{l=1}^{L} EP_l(x), \;\; EP_l(x) = \left(\kappa_l(x)\right)^{x/T} \Pr_l(x), \\
&F_0(x \pm \Delta) = \sum_{l=1}^{L} \left(\kappa_l(x \pm \Delta)\right)^{\pm \Delta/T} \left(\kappa_l(x \pm \Delta)\right)^{x/T} \Pr_l(x, \Delta), \\
&\Pr_l(x, \Delta) = \sum_{k=1}^{K} \left[Ac_k^{(l)}(\pm\Delta) \cos\left(2\pi k \frac{x}{T_x}\right) + As_k^{(l)}(\pm\Delta) \sin\left(2\pi k \frac{x}{T_x}\right) \right],
\end{aligned} \tag{A2-1}$$

where

$$\begin{pmatrix} Ac_k^{(l)}(\pm\Delta) \\ As_k^{(l)}(\pm\Delta) \end{pmatrix} = \begin{pmatrix} \cos\left(2\pi k\left(\frac{\Delta}{T_x}\right)\right) & \pm\sin\left(2\pi k\left(\frac{\Delta}{T_x}\right)\right) \\ \mp\sin\left(2\pi k\left(\frac{\Delta}{T_x}\right)\right) & \cos\left(2\pi k\left(\frac{\Delta}{T_x}\right)\right) \end{pmatrix} \cdot \begin{pmatrix} Ac_k^{(l)} \\ As_k^{(l)} \end{pmatrix}, \qquad \text{(A2-2)}$$

where the last expression represents the rotation matrix which connects the previous decomposition coefficients $Ac_k^{(l)}, As_k^{(l)}$ with the new ones. The same rotation property holds true for the functions $\kappa_l(x \pm \Delta) = \kappa_l(x, \Delta)$ because they are supposed to be periodical also alongside with the functions $Pr_l(x, \Delta)$. As one can notice from expression (A2-1), the variables x and Δ are *separated* and one receives a possibility to consider the shifted function $F(x + \Delta)$ staying in the *initial* observation interval for the input variable x. To avoid misunderstanding we should stress here that the shifting value Δ represents an *independent* variable and does not depend on index l.

Acknowledgements

The authors[4)] thank the support of academic exchanges from “High-end Experts Recruitment Program” of Guangdong province, China. The authors appreciate the support of the research project from the grant "3D Ultrasound magnetic locating of parturition monitoring by fractal-dynamic signal processing" of the Guangdong Scientific Planning Program (No. 2014A050503046) in the frame of JNU-KNRTU(KAI) Joint-Lab. "FracDynamics and Signal Processing".

References

[1] R.R. Nigmatullin, W. Zhang and D. Striccoli. General theory of experiment containing reproducible data: The reduction to an ideal experiment. *Communications in Nonlinear Science and Numerical Simulation*, 27, (2015), pp 175-192.

[2] L.R. Rabiner and B. Gold, "Theory and application of digital signal processing". Englewood Cliffs, NJ, Prentice-Hall, Inc., 1975.

[3] Singleton Jr, A. Royce, B.C. Straits, and M. M. Straits, "Approaches to social research". Oxford University Press, 1993.

[4] J. M. Mendel, "Lessons in estimation theory for signal processing, communications, and control". Pearson Education, 1995.

[5] M.T. Hagan, H. B. Demuth and M. H. Beale, "Neural network design". Boston: Pws Pub., 1996.

[6] E.C. Ifeachor, and B.W. Jervis, "Digital signal processing: a practical approach". Pearson Education, 2002.

[7] D.C. Montgomery, C.L. Jennings and M. Kulahci, "Introduction to time series analysis and forecasting". John Wiley & Sons, 2011.

[8] J.S. Bendat and A.G. Piersol, "Random data: analysis and measurement procedures". John Wiley & Sons, 2011.

[9] A. Gelman, J.B. Carlin, H.S. Stern, D.B. Dunson, A. Vehtari and D.B. Rubin, "Bayesian data analysis". CRC press, 2013.

[10] G. E.P. Box, G.M. Jenkins and G.C. Reinsel, "Time series analysis: forecasting and control". John Wiley & Sons, 2013.

[11] Raoul R. Nigmatullin, Vyacheslav A. Toboev, Paolo Lino, Guido Maione. Reduced fractal model for quantitative analysis of averaged micromotions in mesoscale: Characterization of blow-like signals. *Chaos, Solitons & Fractals,* 76 (2015) pp. 166–181.

[12] J. Kwapien, S. Drozdz, Physical approach to complex systems, Physics Reports 515 (2012) 115.

[13] M. Maric, "Sensor for Injection Rate Measurements", *Sensors*, 2006, 6, 1367-1382.

[14] A. I. Ramírez, S. Som, T. P. Rutter, D. E. Longman, S. K. Aggarwal, "Investigation of the Effects of Rate of Injection on Combustion Phasing and Emission Characteristics: Experimental and Numerical Study", Spring Technical Meeting of the Central States Section of the Combustion Institute, April 22–24, 2012.

[15] S. Vass, H. Németh, "Sensitivity analysis of instantaneous fuel injection rate determination for detailed Diesel combustion models", *Transportation Engineering*, 41/1 (2013) 77–85.

[16] W. Bosch, "The Fuel Rate Indicator: A New Measuring Instrument For Display of the Characteristics of Individual Injection", SAE Technical Paper 660749, 1966.

[17] R. Nigmatullin, R. Rakhmatullin. Detection of quasi-periodic processes in repeated-measurements: New approach for the fitting and clusterization of different data. *Communications of Nonlinear Science and Numerical Simulation* **19** (2014) pp. 4080-4093.

[18] R.R. Nigmatullin, A.A. Khamzin and J. T. Machado, Detection of quasi-periodic processes in complex systems: how do we quantitatively describe their properties? *Physica Scripta* **89** (2014) 015201 (11pp).

[19] Raoul R. Nigmatullin, Sergey I. Osokin, Dumitru Baleanu, Sawsan Al-Amri, Ameer Azam, Adnan Memic, The First Observation of Memory Effects in the InfraRed (FT-IR) Measurements: Do Successive Measurements Remember Each Other? *PLoS ONE*, Open access journal, April 9 (4) (2014) e94305.

[20] Raoul R. Nigmatullin, José Tenreiro Machado, Rui Menezes. Self-similarity principle: the reduced description of randomness. *Central European Journal of Physics*. **11**(6) (2013) P 724-739. (DOI: 10.2478/s11534-013-0181-9).
[21] R.R. Nigmatullin, R.M. Rakhmatullin, S.I. Osokin, How to reduce reproducible measurements to an ideal experiment? Magnetic Resonance in Solids, Electronic Journal, (2014) **16** (2) pp.1-19. http://mrsej.kpfu.ru.

Figure(s)

Click here to download Figure(s): Figs_all_(fv).docx

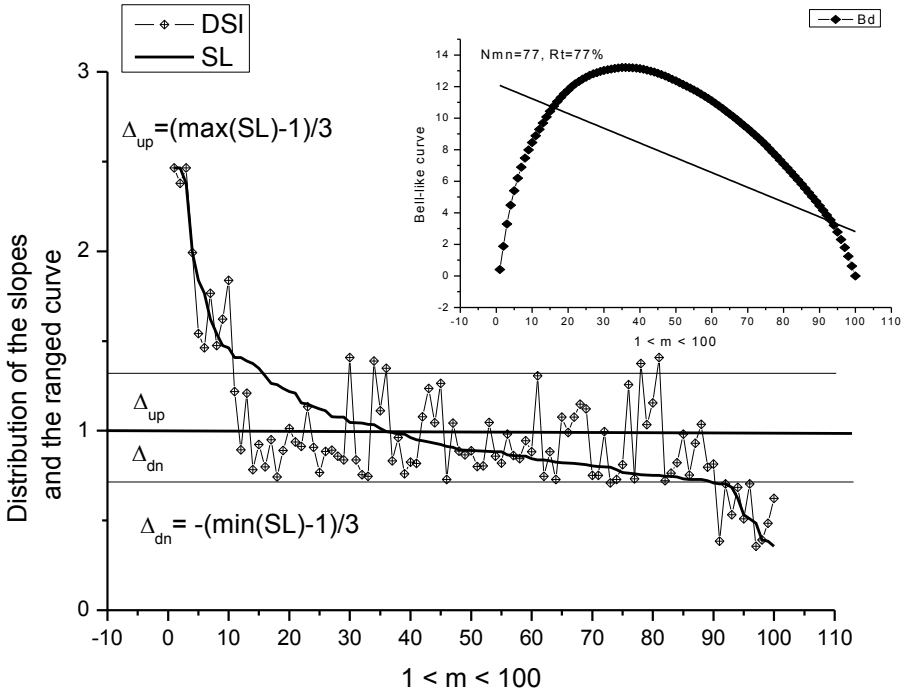

Fig.1(a). These plots illustrate the idea of separation of all measurements (including the corresponding equipment) on three classes (clusters). Here most of the slopes (77) are located in the vicinity of unitary slope. If we divide all values of the ranged slopes (marked as SL) on three intervals (min(SL), $1-\Delta_{dn}$) ($1-\Delta_{dn}$, $1+\Delta_{up}$), ($1+\Delta_{up}$, max(SL)), then 77% of measurements score in the central interval. So, they can be characterized as "good" measurements in accordance with the proposed criterion.

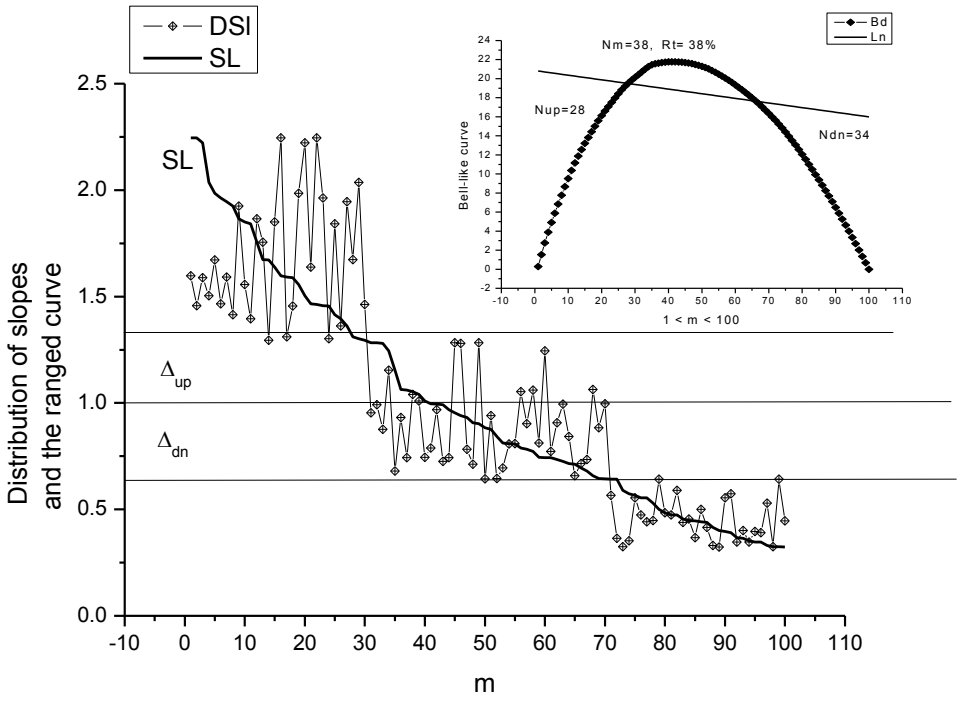

Fig.1(b). Here the selection on three intervals remains the same $\Delta_{up}=(\max(SL)-1)/3\approx\Delta_{dn}=(1-\min(SL))/3$, but the number *Nmn* entering in the central interval is 38. So, these measurements can be characterized as "acceptable".

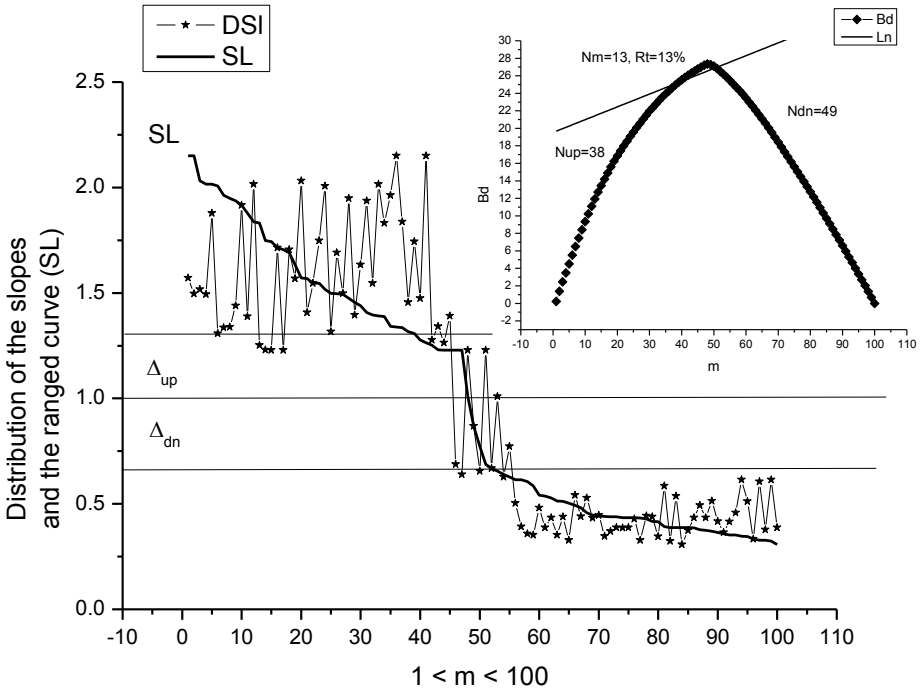

Fig.1(c). Here we show the case of "bad" measurements. The value of *Nmn*=13 and most of measurements are located in "up" (*Nup*=38) and "dn" (*Ndn*=49) regions, correspondingly.

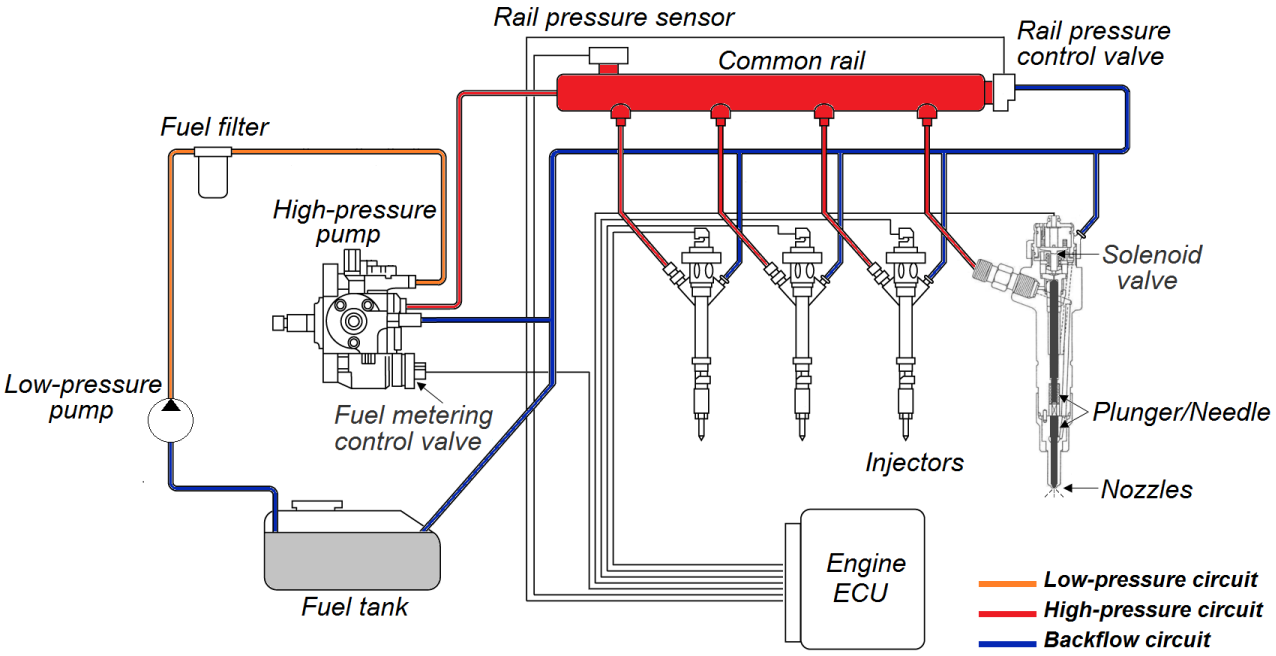

Fig. **2**: The Common Rail Injection System

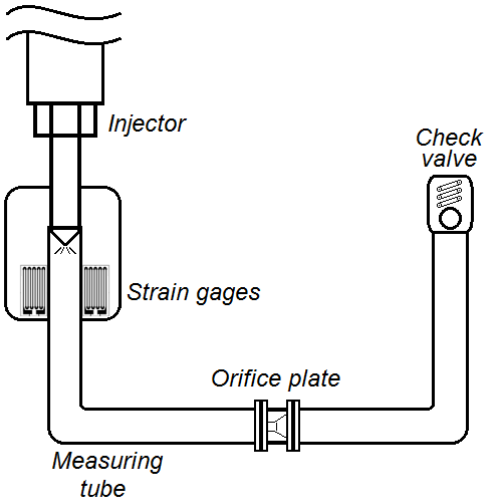

Fig. 3: Scheme of the Bosch Rate of Injection Meter

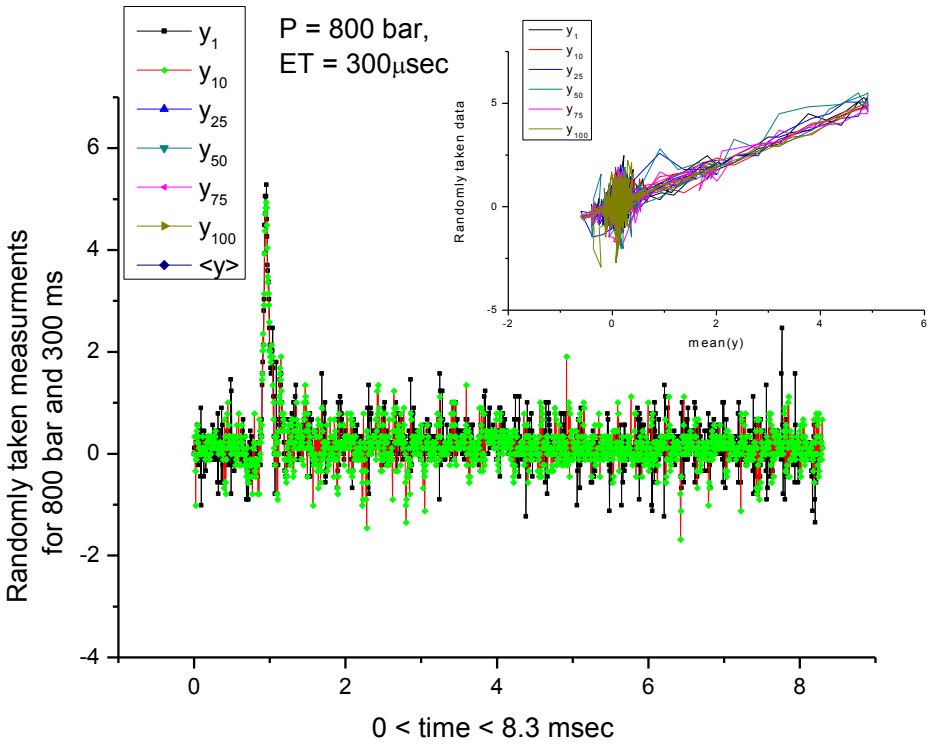

Fig. 4. This plot demonstrates real injection data measured at a rail pressure of 800 bar and with energizing time (ET) of 300 μs. We show only 6 randomly taken data together with the mean value <*y*>. The total number of measurements is *M*=100. The plots of these data with respect to <*y*> demonstrate their strong correlations (see small figure above).

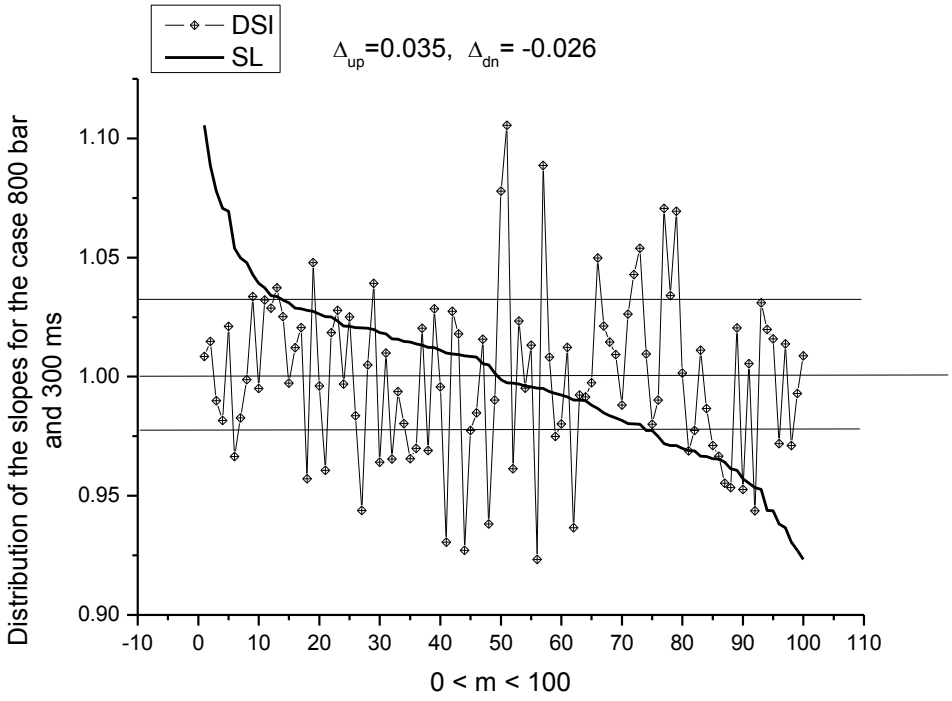

Fig.5(a). Distribution of the slopes corresponding to *M* = 100 measurements for P = 300 bar, ET = 300μs.

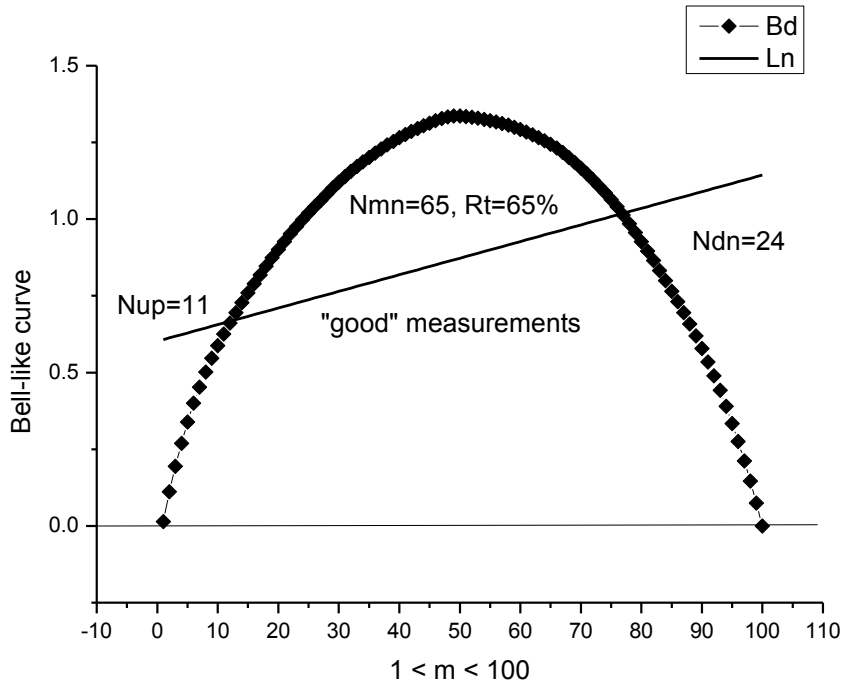

Fig.5(b). The bell-like curve corresponding to the distribution shows that Rt=65% of measurements scored into the central interval. So, they can be characterized as "good" measurements.

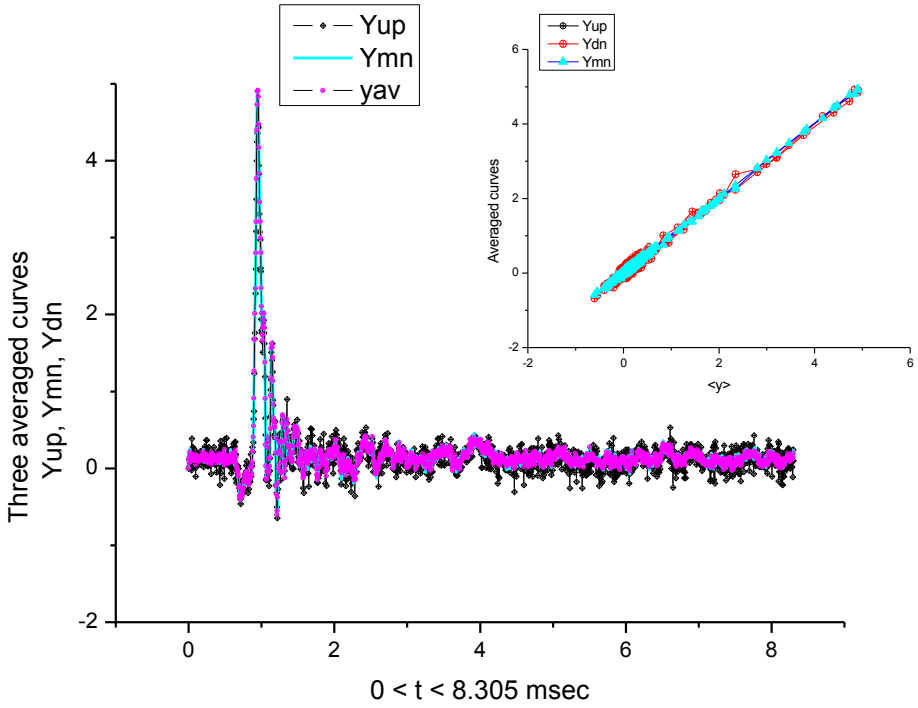

Fig.6. This plot shows the results of the clusterization procedure. Instead of 100 successive measurements we receive only 3 averaged and strongly correlated (see the upper plot) measurements that are very close to each other. We select only the mean measurement *Ymn*(*x*) for the realization of the further fitting procedure.

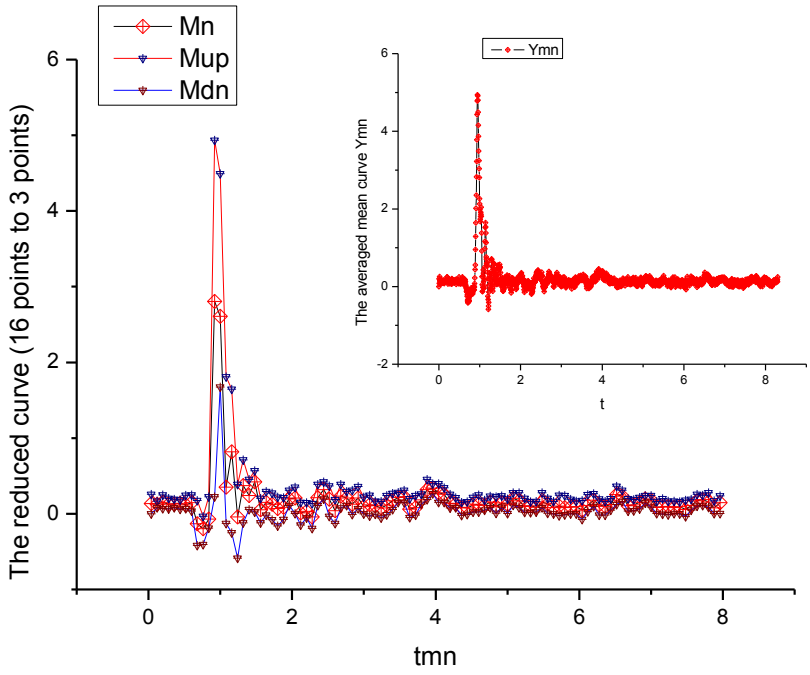

Fig.7. Here we show the result of the reduction procedure. 16 points of the initial curve *Ymn* are reduced to three incident (with invariant relatively permutations) points. The curve *Mn* reflects the distribution of mean values, *Mup* the maximal values and *Mdn* the minimal values for each segment, correspondingly. The number of segments is determined as the integer part of the ratio $R = L(1660)/b(16) = 100$. The value *tmn* is determined as a mean value of time corresponding to each chosen interval.

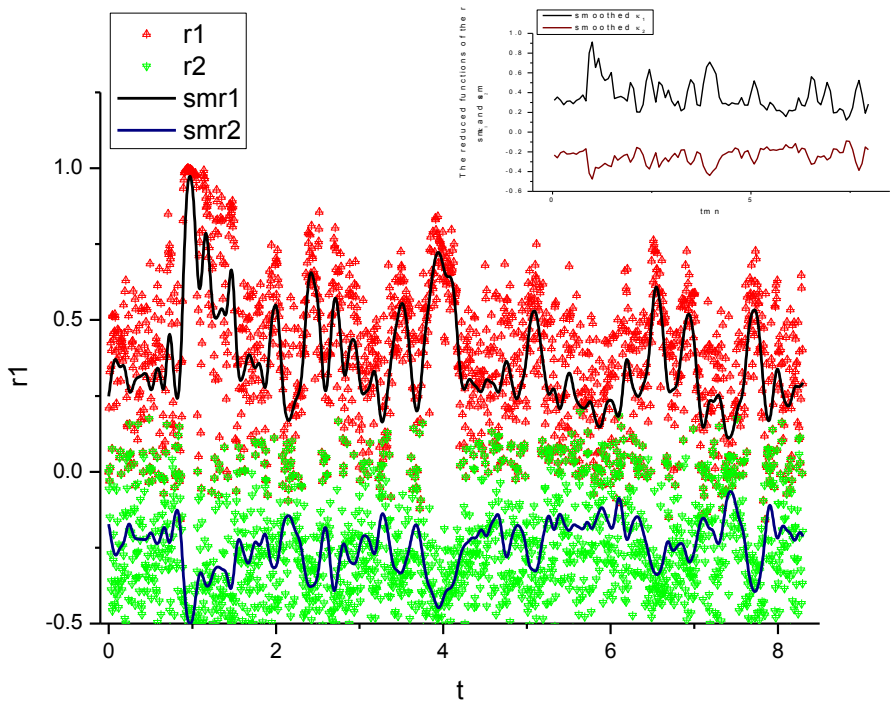

Fig.8. Here we demonstrate the behavior of the roots $\kappa_{1,2}$ and their smoothed values (shown by solid lines). On the upper plot we show the reduced values of the smoothed roots. These functions can be used for the fitting of the *Mn* function shown on the previous figure.

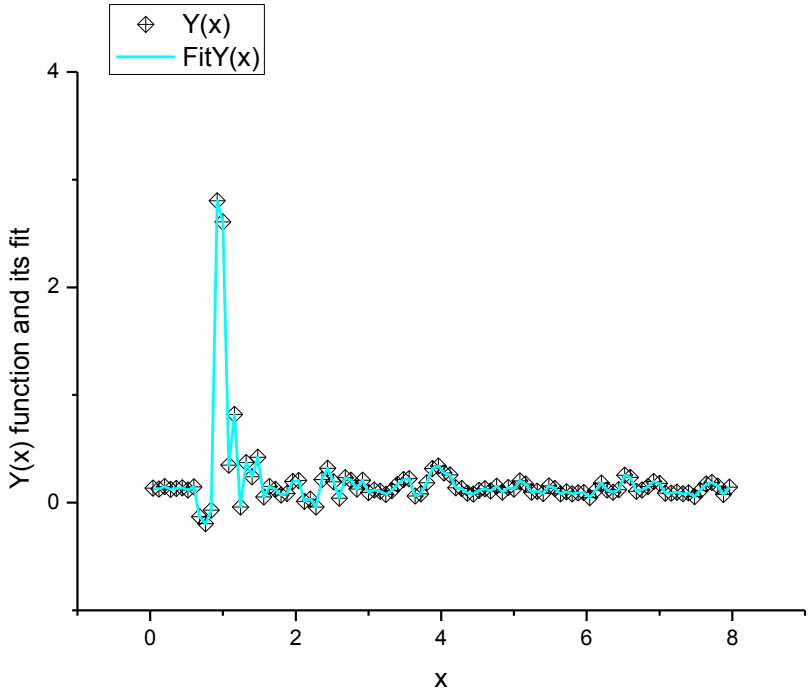

Fig.9. The fitting of the function $Y(x)$ ($Y = Mn$, $x = tmn$) with the help of expression (18). This function can be fitted with very high accuracy (*RelErr* < 0.01%). The amplitude-frequency response (AFR) serves as an intermediate model (IM) of this function.

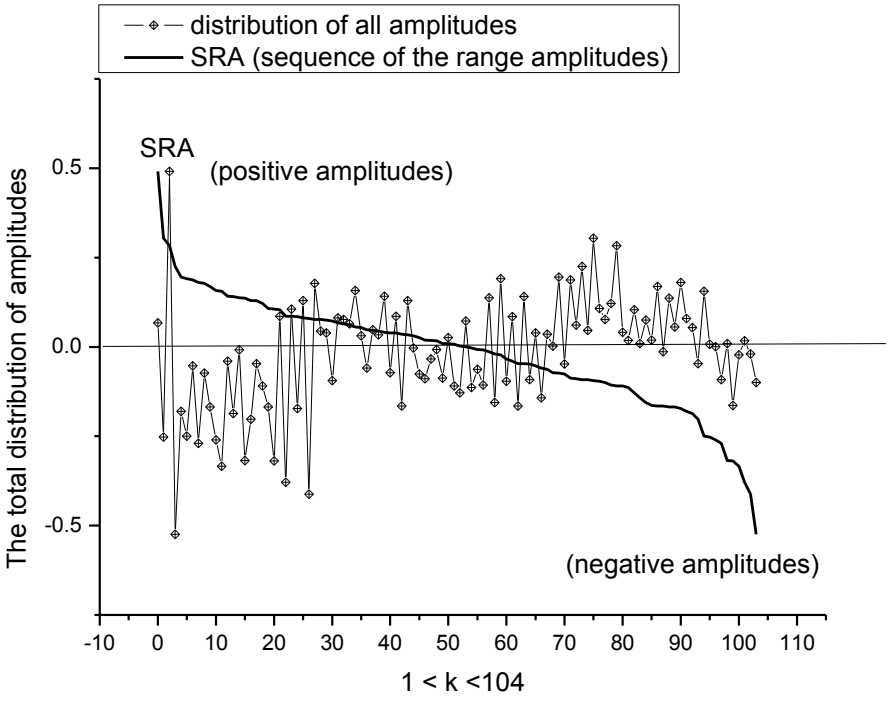

Fig. 10(a). This plot demonstrates the distribution of all amplitudes $A_0, Ac_k^{(1,2)}(x), As_k^{(1,2)}(x)$ that enter to expression (18). We note that the number of these amplitudes are comparable with number of the reduced points (R=100) that provides the practical coincidence of the fitting curve with $Y(x)$.

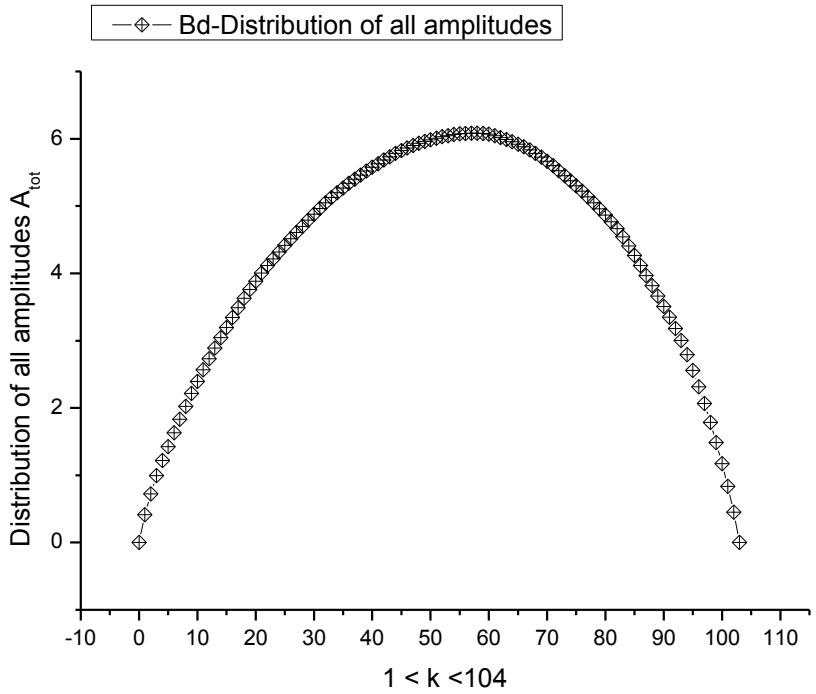

Fig. 10(b). This curve is very useful in analysis of distribution of all amplitudes (shown on the previous figure) when the number of this amplitudes are relatively large (>100). This distribution can be fitted with the help of the function (12) and can be "read" in terms of 4 fitting parameters. The maximal value of this bell-like curve corresponds to the amplitude having the minimal value.

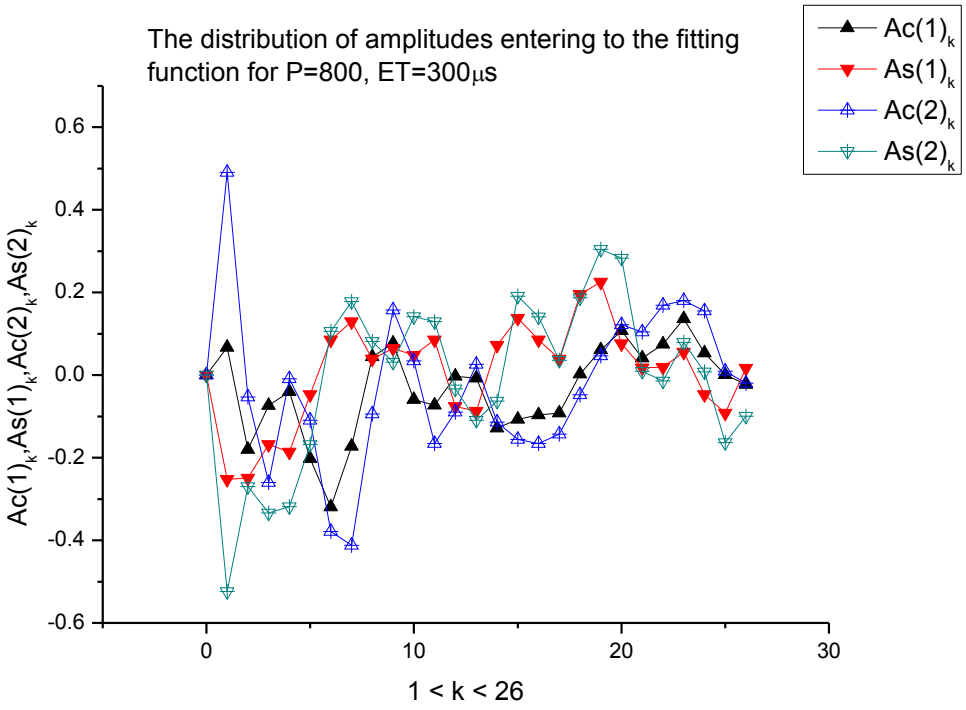

Fig.10(c). The separate distribution of the amplitudes $Ac_k^{(1,2)}(x), As_k^{(1,2)}(x)$ that enter into the fitting function (18).

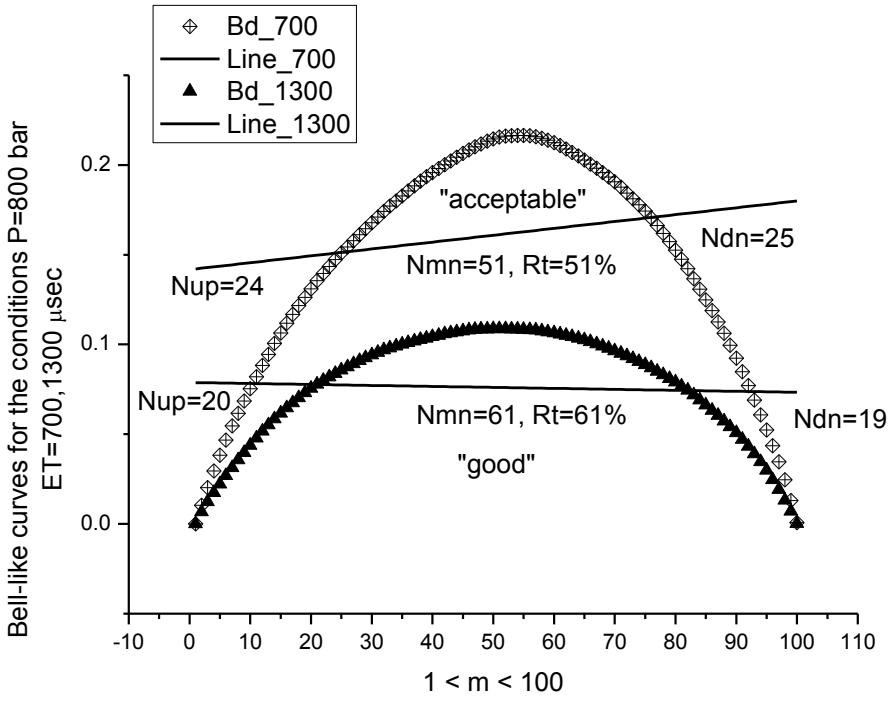

Fig.11. Here we show the bell-like curves for two set of measurements corresponding to 700μs (upper curve) and 1300μs. The bell-like curve depicted on Fig.5(b) cannot be placed here because its range is high. Here we want to say that the maximal value of this curve reflects the range of the measurements with respect to the slope having the unit value. The minimal range corresponds to 1300μs and, correspondingly, the maximal value corresponds to the ET=300μs (Fig.5(b)). The quality of the performed measurements in accordance with classification (13) is shown also.

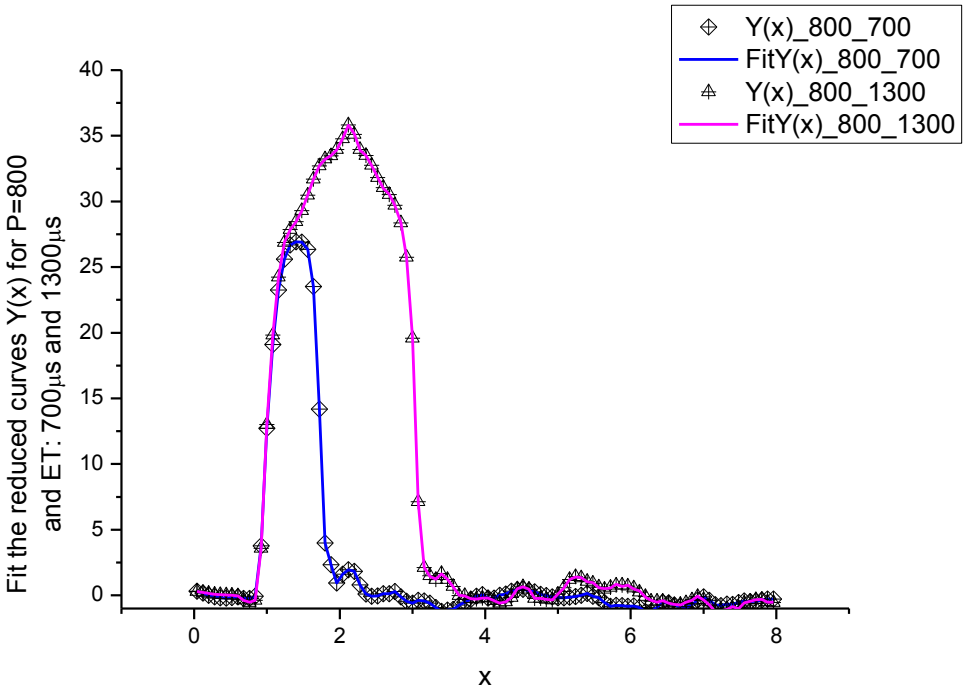

Fig.12. Here we demonstrate the fit for the reduced curves corresponding to mean values and realized with the help of the procedure described in the stage 3 for ET=700 and 1300 μs, correspondingly. The fitting curve depicted on Fig.9 (because of the big difference of their ranges) cannot be placed here.

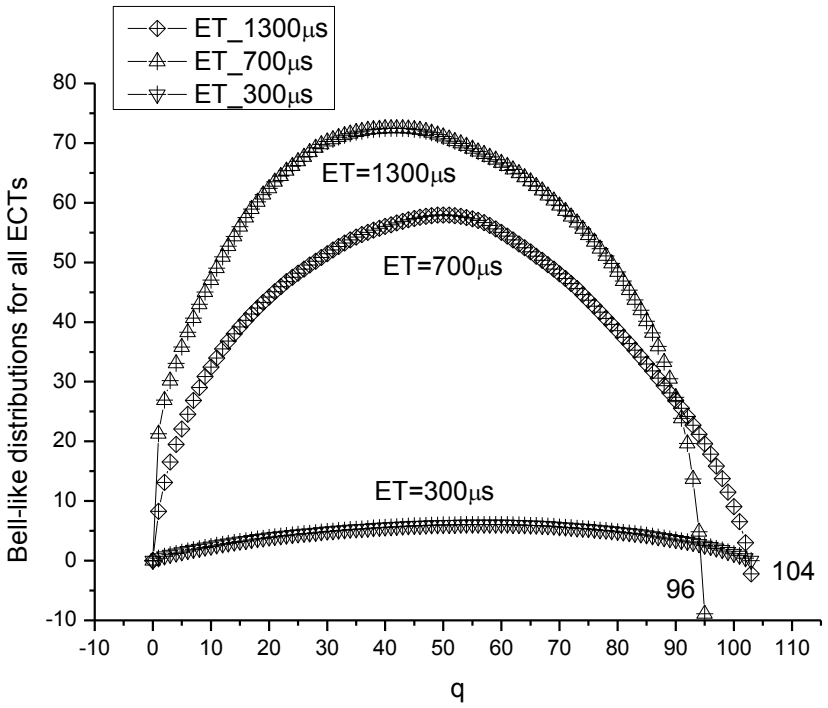

Fig.13(a). The total distribution of the amplitudes $Ac_k^{(1,2)}(x), As_k^{(1,2)}(x)$ calculated for all ETs. This plot is informative when the number of modes is high (>100) and it is necessary to evaluate the corresponding spectrograms in general. One can notice here that the amplitudes figuring in the fitting function (18) increase with increasing the value of the energizing time.

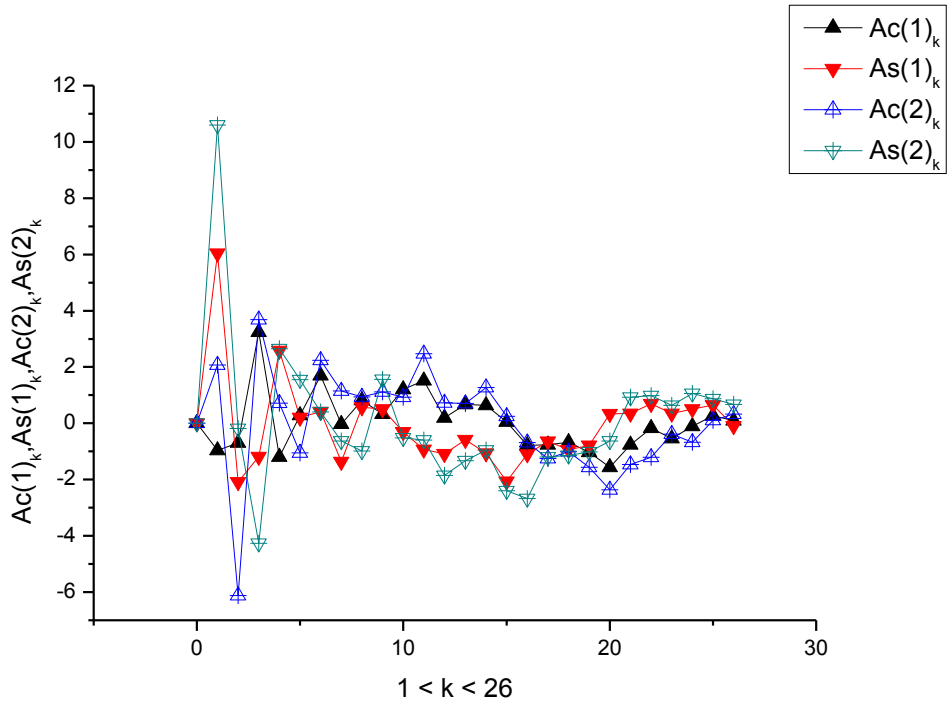

Fig.13(b). The separate distribution of the amplitudes $Ac_k^{(1,2)}(x), As_k^{(1,2)}(x)$ that enter into the fitting function (18) for P=800 bar, ET=700μs.

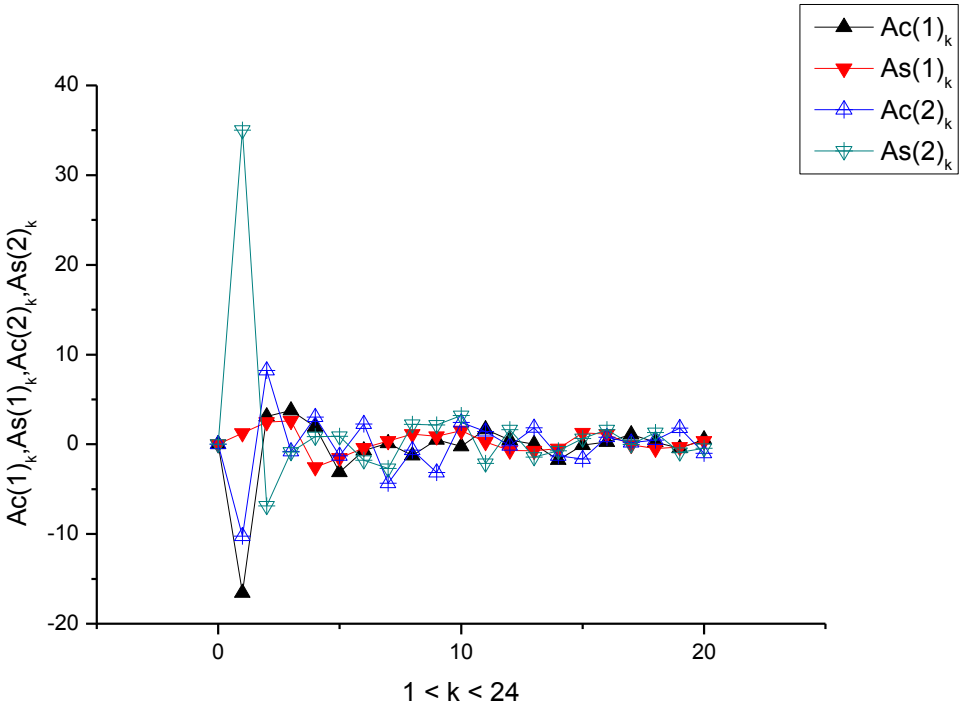

Fig.13(c). The separate distribution of the amplitudes $Ac_k^{(1,2)}(x), As_k^{(1,2)}(x)$ that enter into the fitting function (18) for P=800 bar, ET=1300μs.

Table(s)

Table of additional fitting parameters that enter to the fitting function (18)

ET(μs)	$T_{optimal}$	ln(mean(κ_1))	ln(mean$\lvert(\kappa_2)\rvert$)	A_0	Range(A_{tot})	RelErr(%)	K
300	4.24	-0.99862	-1.40454	0.67379	1.01499	8.68702E-5	26
700	4.24	-0.99862	-1.40454	0.22757	16.7135	9.22558E-5	26
1300	4	-0.99862	-1.40454	9.02344	51.6305	0.44392	24

The range of the function is determined conventionally as the difference between the maximal and minimal values i.e.: Range (F) = max(F) – min(F). The relative error is determined by expression